Catalysis Today 158 (2010) 343–347

Contents lists available at ScienceDirect

Catalysis Today

journal homepage: www.elsevier.com/locate/cattod

Upgrading of light cycle oil via coupled hydrogenation and ring-opening over NiW/Al_2O_3-USY catalysts

Liang Wang[a], Baojian Shen[a,*], Fang Fang[a], Fucun Wang[b], Ran Tian[b], Zhihua Zhang[b], Lishan Cui[a]

[a] State Key Laboratory of Heavy Oil Processing, The Key Laboratory of Catalysis of CNPC, Faculty of Chemical Science and Engineering, China University of Petroleum, 18# Fuxue Rd., Beijing, Changping 102249, China
[b] Daqing Chemical Engineering Research Center, Petrochemical Research Institute of PetroChina Company Limited, Daqing 163714, China

ARTICLE INFO

Article history:
Available online 13 May 2010

Keywords:
Light cycle oil
Tetralin
Hydrogenation
Ring-opening
USY zeolite
Acidity

ABSTRACT

A series of ultrastable Y (USY) zeolite samples with different acidities and pore sizes are prepared via hydrothermal and acid treatments. NiW sulfide catalysts are maintained on a mixed support of USY zeolite and Al_2O_3. The catalytic coupled hydrogenation and ring-opening performance are studied on a continuous fixed-bed reactor using tetralin as the model compound. All catalysts show high tetralin conversions under the reaction conditions studied [T = 613 K, P = 4.0 MPa, LHSV = 2.0 h^{-1}, H_2/oil (v/v) = 500]. Product yields and selectivity are mainly determined by the zeolite property (i.e., acidity). A medium to strong zeolite acidity is the key factor in the ring-opening selectivity of tetralin. A maximum high cetane ring-opening product yield of 39.1 wt% is obtained at a C_{10} yield of 98.2 wt% for a USY zeolite with medium acidity. Using an fluid catalytic cracking light cycle oil feedstock, the activity of the catalyst is higher than that of commercial catalysts, giving a 14-unit cetane number increase at a diesel yield of 97.6 wt%. Because the first step of the ring-opening reaction is hydrogenation, the catalyst must have high hydrogenation activity. The WS_2 slabs have a high average layer number of 2.7 on the catalyst using the support presented here.

1. Introduction

Light cycle oil (LCO) from fluid catalytic cracking (FCC) is becoming an important source for diesel pools. It is characterized by a high polyaromatic content and low cetane number. Several approaches have been proposed to improve the cetane number, including the use of cetane boosters [1], blending with Fischer–Tropsch gas-to-liquid diesel fuels [2], deep hydrotreating [3], hydrocracking [4], and selective ring-opening (SRO) [5]. In contrast to conventional hydrocracking, selective ring-opening requires that only one C–C bond in the naphthenic molecule be broken, thus preventing significant molecular weight reduction of the feed.

Selective ring-opening can be carried out on certain noble metals by hydrogenolysis. The hydrogenolysis ability of these catalysts increases in the order of: Pt < Rh < Ir < Ru [6–8]. The ring-opening of naphthenes can also take place through an acid-catalyzed process performed primarily on zeolites. The activity is reportedly dependent on the number and strength of Brønsted acid sites and porosity of the support [9,10]. Thus, the best ring-opening results are obtained from zeolites exhibiting medium acidity. The use of zeolites with large pores favors the ring-opening reaction [11–13].

Ring-opening reactions are enhanced by the use of bifunctional catalysts [14]. The judicious control of the metal to acid ratio in a given catalyst is important. The formation of the ring-opening products increases with increasing proximity between Pt and the acid sites [15]. Thus, a close relationship between the metal and acid sites is necessary for improvement of bifunctional catalysts in the ring-opening reaction.

Numerous studies have been conducted on the use of noble metal catalysts, but they are costly and easily poisoned by sulfur compounds [15–17]. These catalysts have to be used in a multi-stage process. Metal sulfide catalysts are able to catalyze the ring-opening reaction in the presence of sulfur compounds. However, few studies have focused on these materials. In this paper, we investigate the use of mixed ultrastable Y (USY) zeolite and Al_2O_3 to support sulfided NiW-based catalysts for the hydrogenation and ring-opening of tetralin and the hydrotreatment of LCO. The influences of the acidity and pore size of USY zeolite are also studied. The correlations between the catalytic activity and structures of NiW sulfide on the support are further investigated.

2. Experimental

The USY zeolite was prepared from the starting NaY sample by ammonium exchange, followed by subsequent hydrothermal and acid treatment. By changing the treatment conditions, three

* Corresponding author. Tel.: +86 10 89733369; fax: +86 10 89733369.
E-mail addresses: baojian@cup.edu.cn, baojian2004@yeah.net (B. Shen).

0920-5861/$ – see front matter © 2010 Elsevier B.V. All rights reserved.
doi:10.1016/j.cattod.2010.04.018

kinds of USY samples were obtained. The support was prepared by mixing zeolite and pseudo-boehmite. The resulting compound was extruded to form a cylindrical extrudate, which was dried overnight at 383 K and then calcined in the air at 823 K for 4 h. The composite support obtained was designated as AUSY. NiW catalysts with a load of 4 wt% NiO and 27 wt% WO_3 were prepared via the pore volume co-impregnation method with an aqueous solution of ammonium metatungstate and nickel nitrate. The catalyst was dried overnight at 393 K and calcined at 753 K for 4 h. As a reference catalyst without zeolite, an Al_2O_3-supported NiW catalyst with the same NiO and WO_3 loads was prepared.

X-ray diffraction (XRD) patterns were recorded on a Shimadzu-6000 diffractometer using Cu Kα radiation at 40 kV and 30 mA. The porosity of each sample was determined by measuring the N_2 isotherm at 77 K with a Micromeritics ASAP 2020 automated system. The total surface area was calculated according to the BET isothermal equation, and the micropore volume, the mesopore volume, and external surface area were evaluated by the *t*-plot method. The pore size distribution profile was calculated using the BJH method with an N_2 desorption isotherm. Ammonia-temperature-programmed desorption (NH_3-TPD) of the zeolites was performed using Quantachrome Autosorb-1 equipped with a thermal conductivity detector (TCD) to monitor the exit gas. The morphology of the NiW sulfide was observed by high resolution transmission electron microscopy (HRTEM) on a Tecnai G^2 F20 field emission machine operated at 200 kV. Samples were prepared by the drop method.

The coupled hydrogenation and ring-opening of tetralin was evaluated in a continuous flow fixed-bed micro-reactor under the following conditions: a model feed of 10 wt% tetralin in decane, a catalyst load of 1.0 g, a reaction pressure of 4.0 MPa, a reaction temperature of 613 K, a feed flow rate of 3.62 mL/h, and an H_2/oil ratio of 500 (v/v). The catalysts were first pre-sulfided in situ with a sulfiding feed of 10 vol% CS_2 in decane at 4.0 MPa and 603 K for 4 h. After steady-state conditions were reached, the liquid effluents were periodically collected and measured on an SP 3420 gas chromatograph (GC) using a flame ionization detector and a DM-5 capillary column (30.0 m × 0.25 mm × 0.32 μm). Identification of the reaction products was accomplished by mass spectrometry (MS) and by a comparison of the retention times with those of available standard mixtures. The GC patterns obtained from our study were compared with those in Sato's work [18]. To facilitate the discussion, reaction products were grouped as follows: (a) light paraffins, composed mainly of propane and isobutene; (b) light naphthenes with less than 10 carbon atoms; (c) decalin; (d) decalin isomers or isodecalins having one or two C_5 naphthenic rings; and (e) ring-opening products, composed mainly of *n*-butylbenzene and *iso*-butylbenzene having the same number of carbon atoms as the aromatic reactant (C_{10}). These are the most important products from the point of view of cetane number.

The hydrotreatment of the catalysts was conducted in a 20 mL continuous flow fixed-bed reactor using Daqing FCC LCO as the feed. The length of the catalyst was 2–3 mm, and the catalyst loading volume was 20 mL. The catalysts were first pre-sulfided in situ with a sulfiding feed of 2 wt% CS_2 in kerosene. The reaction operating conditions were 8.0 MPa, 633 K, an LHSV of 1 h^{-1}, and an H_2/oil ratio of 800 (v/v). The reaction products were condensed and periodically separated from a gas–liquid separator. After the feedstocks were treated for about 5 days, the liquid products were collected and analyzed. The diesel cut boiling range was found to be 453–633 K. The nitrogen and sulfur contents in the samples were analyzed according to ASTM D4629 and ASTM D4294, respectively. The total aromatic content was determined by the standard fluorescence indicator adsorption (FIA). The cetane number was determined via diesel engine testing.

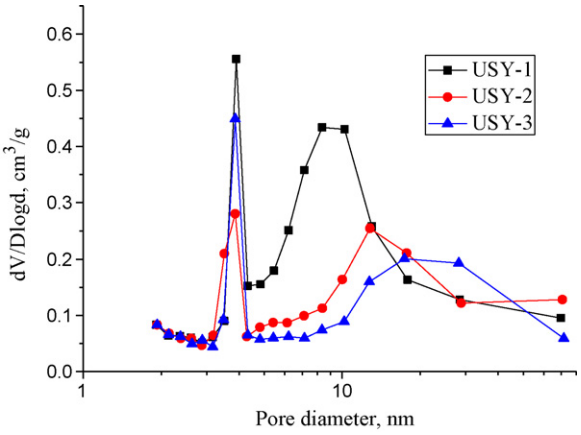

Fig. 1. Pore size distribution of the zeolites.

3. Results and discussion

3.1. Characterization of zeolites

The textural properties of the zeolites determined by N_2 adsorption are shown in Table 1.

The BET surface area (S_{BET}) increases in the order of: USY-1 < USY-2 < USY-3. The same trends can be observed for the micropore surface area (S_{micro}), total pore volume (V_p), and micropore volume (V_{micro}) of the zeolites. The results clearly show that the micropore properties of USY-3 are preserved well. The external surface area (S_{exter}) and the mesopore volume (V_{meso}) of USY-3 are also the highest obtained. Sato et al. claimed that mesopore structures can influence the interaction between zeolite and NiW sulfide and the catalytic performance of the USY-based hydrocracking catalyst [19]. As such, precise control of the mesopore structures is required. USY-1 has the largest average pore diameter (D_{aver}).

Fig. 1 shows the pore size distribution profiles of the zeolites. All USY zeolites have two peaks at about 3.8 and 15 nm. The former is related to the mesoporosity created during the dealuminization procedure used to obtain high-silica faujasites [20], while the latter is attributed to the void spaces among the particle agglomerates. The intensity of the peaks at about 3.8 nm decreases in the order of: USY-1 > USY-3 > USY-2.

Fig. 2 shows the NH_3-TPD profiles of the zeolites. The TPD profile of USY shows a single peak at about 460 K. The peak areas of the NH_3-TPD curves decrease in the order of: USY-3 > USY-2 > USY-1. The use of zeolites with medium acidity favors ring-opening reactions [9].

Table 1
Textural properties of the zeolites.

Sample	S_{BET} (m^2/g)	S_{micro} (m^2/g)	S_{exter} (m^2/g)	V_p (cm^3/g)	V_{micro} (cm^3/g)	V_{meso} (cm^3/g)	D_{aver} (nm)
USY-1	396	306	90	0.38	0.16	0.22	3.88
USY-2	595	531	64	0.45	0.27	0.18	3.05
USY-3	731	605	126	0.61	0.29	0.32	3.32

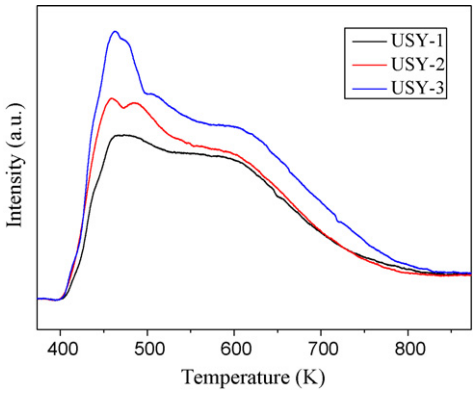

Fig. 2. NH_3-TPD profiles of the zeolites.

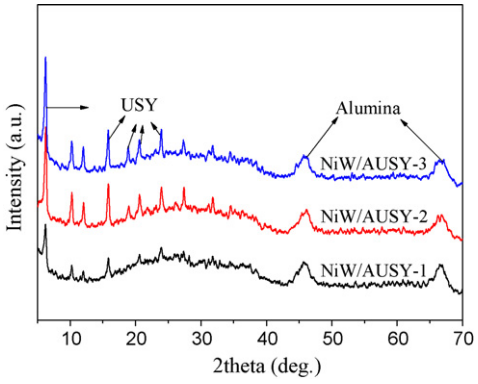

Fig. 3. XRD profiles of the catalysts.

3.2. Characterization of catalysts

The XRD patterns of the catalysts are shown in Fig. 3. The characteristic diffraction peaks of zeolite Y and Al_2O_3 are marked in the figure. After impregnation with nickel and tungsten, no obvious metal oxide peak is found in the XRD patterns of all the catalysts. The intensities of the diffraction peaks of Al_2O_3 are virtually the same for all samples.

Table 2
Textural properties of the catalysts.

Items	NiW/AUSY-1	NiW/AUSY-2	NiW/AUSY-3	NiW/Al_2O_3
Surface area (m^2/g)	188	216	216	163
Pore volume (mL/g)	0.27	0.29	0.28	0.26
Average pore size (nm)	5.78	5.31	5.13	6.34

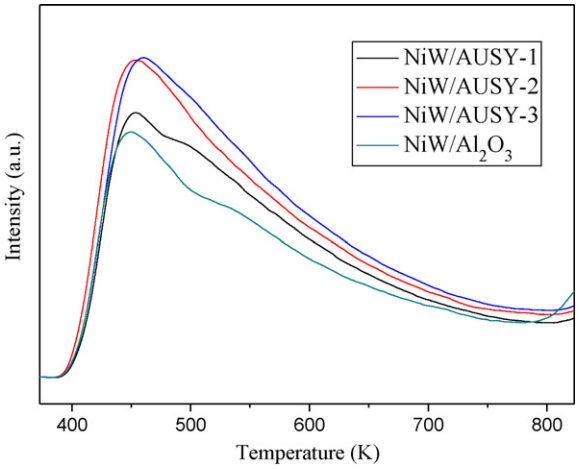

Fig. 4. NH_3-TPD profiles of the catalysts.

The textural properties of the catalysts are listed in Table 2. As expected, the surface areas of the catalysts containing zeolites increase when the zeolites are introduced to the catalyst support. NiW/AUSY-3 displays the highest surface area among the four catalysts due to the maximum surface area of USY-3. The introduction of zeolite to the catalyst support results in small average pore sizes.

Fig. 4 shows the NH_3-TPD profiles of the catalysts. The TPD profile of the catalyst contains a single peak at about 460 K. The peak areas of the NH_3-TPD curves decrease in the order of: NiW/AUSY-3 > NiW/AUSY-2 > NiW/AUSY-1 > NiW/Al_2O_3. The order is the same as that of the acidity of their support materials. The addition of zeolite Y results in a significant increase in total acidity.

The representative TEM images of the sulfided catalysts are illustrated in Fig. 5.

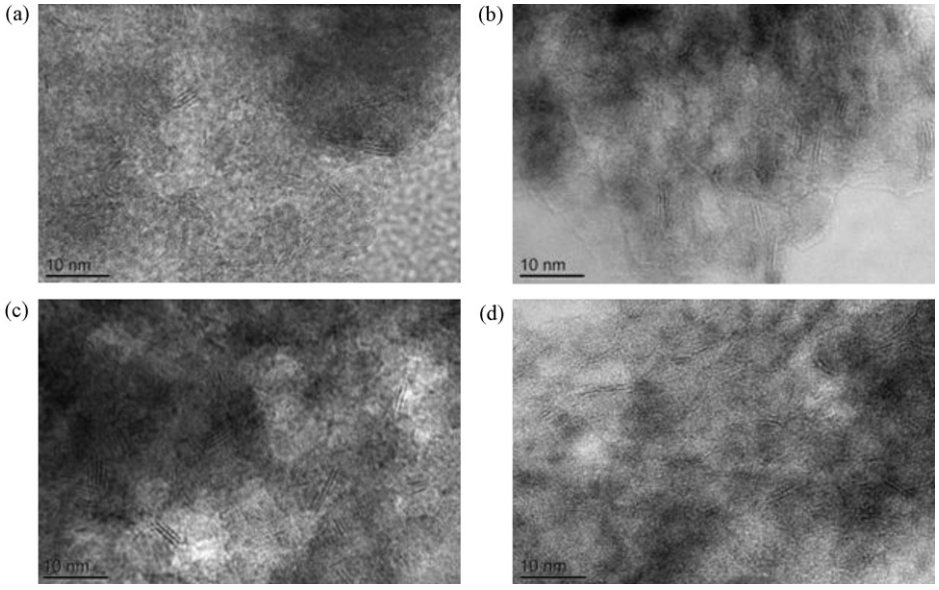

Fig. 5. TEM images of (a) NiW/AUSY-1, (b) NiW/AUSY-2, (c) NiW/AUSY-3, and (d) NiW/Al_2O_3.

Table 3
Average number and lengths of the WS_2 layers for sulfided catalysts.

Items	NiW/ AUSY-1	NiW/ AUSY-2	NiW/ AUSY-3	NiW/ Al_2O_3
Average number of layers	2.3	2.7	2.7	2.0
Average length of slabs (nm)	3.73	3.82	3.70	3.69

The TEM images reveal the presence of typical structures of the layered WS_2 phase. This was also confirmed by energy dispersive X-ray spectroscopy (EDX). No large aggregates of WS_2 are observed in the TEM. For WS_2 on the catalysts, the average number of layers per slab and average length of slabs are calculated from measurements of about 300 crystallites [21]. The statistical average lengths and number of the layers of the WS_2 slabs are given in Table 3. Compared with NiW/Al_2O_3, catalysts containing zeolites exhibit higher average numbers of layers. NiW/AUSY-2 and NiW/AUSY-3 have the same average number of layers, which is higher than that of NiW/AUSY-1. Multilayered WS_2 slabs provide higher multivacancy density compared with single-layered or thin slabs. This can facilitate the π-complexation of the aromatic ring on multilayered WS_2 slabs. Consequently, higher stacking numbers of WS_2 slabs favor increases in hydrogenation activity [22]. The four catalysts show similar average slab lengths.

3.3. Reaction performance evaluation

Table 4 shows the tetralin conversion and product yields of different catalysts. Zeolite can significantly enhance tetralin conversion. While the conversion of catalysts containing zeolites is more easily influenced by coke, they still show higher conversions than NiW/Al_2O_3 (without zeolite). The acidity of zeolite can further convert decalins. In addition, zeolite acidity favors the migration of any hydrogen spillover over acid surfaces [23]. The order of tetralin conversion is in agreement with that of the acidity of catalysts.

Only decalins are formed on NiW/Al_2O_3 in the absence of Brønsted acid sites. In contrast, a considerable amount of decalin isomers and ring-opening products are obtained from catalysts containing zeolites. Li claimed that the essential factor controlling ring-opening activity is catalyst acidity [10]. NiW/AUSY-3, which has a high acidity, gives a low C_{10} yield of only 62.9 wt% because the ring-opening products are further cracked into light paraffins and light naphthenes. Light paraffins (<C_{10}), composed mainly of propane and isobutane, shown in Table 4 are hydrocracking products of tetralin. Tailleur found that, in some strong acid sites, the adsorbed material suffers dehydrogenation, cracking, and polymerization reactions. In weak acid sites, the same molecules can follow isomerization, cyclization, and ring-opening reactions [24]. Some authors showed that selectivity for ring-opening products is higher for less acidic catalysts [17,25]. A maximum ring-opening product yield of 39.1 wt% can be obtained over NiW/AUSY-2 with medium acidity. According to a study by Arribas et al. [15], the metal sites of bifunctional catalyst are directly involved in the activation/isomerization of naphthenes and will thus influence the formation of desired ring-opening products. The number of NiW sulfide layers on NiW/AUSY-2 is high. A strong cooperation between the metal sulfides and acid sites on NiW/AUSY-2 leads to high ring-opening activity.

Table 4
Tetralin conversion and product yields of different catalysts[a].

Catalyst	NiW/ AUSY-1	NiW/ AUSY-2	NiW/ AUSY-3	NiW/ Al_2O_3
Tetralin conversion (%)	75.1	77.9	100	54.3
Product yields (wt%)				
Light paraffins (<C_{10})	0.0	0.8	15.9	0.0
Light naphthenes (<C_{10})	0.0	1.0	21.2	0.0
Decalins	0.0	0.0	0.0	54.3
Decalin isomers	38.2	31.7	40.8	0.0
Ring-opening products	36.9	39.1	22.1	0.0
Tetralin	24.9	22.1	0.0	45.7
Total C_{10}'s	100	98.2	62.9	100

[a] Reaction conditions: T = 613 K, P = 4.0 MPa, LHSV = 2.0 h^{-1} and H_2/oil (v/v) = 500.

Table 5
Decane conversion and product yields of different catalysts[a].

Catalyst	NiW/ AUSY-1	NiW/ AUSY-2	NiW/ AUSY-3	NiW/ Al_2O_3
Decane conversion (%)	0.0	0.0	12.0	0.0
Product yields (wt%)				
C_4–C_6 paraffins	0.0	0.0	12.0	0.0
Decane	100	100	88.0	100

[a] Reaction conditions: T = 613 K, P = 4.0 MPa, LHSV = 2.0 h^{-1} and H_2/oil (v/v) = 500.

Table 6
Evaluation of NiW/AUSY-2 and the commercial catalyst using LCO as the feed[a].

	Feedstock FCC LCO	NiW/ AUSY-2	Commercial catalyst
Diesel yield (wt%)		97.6	97.5
Sulfur (μg/g)	920.2	23.9	38.0
Nitrogen (μg/g)	806.3	4.0	10.5
Aromatic (vol%)	56.9	19.8	33.5
Cetane number	25	39	36.5
Cetane number improvement		14	11.5

[a] Reaction conditions: T = 633 K, P = 8.0 MPa, LHSV = 1.0 h^{-1} and H_2/oil (v/v) = 800.

Under the experimental conditions the solvent decane in model feed may be cracked into small molecular compounds. Table 5 shows the decane conversion and product yields of different catalysts. Almost no hydrocracking of decane takes place on NiW/AUSY-1, NiW/AUSY-2 and NiW/Al_2O_3 due to low catalyst acidity. However, on NiW/AUSY-3 with the highest acidity, the decane is cracked into a considerable amount of small molecule compounds which are mainly C_5 paraffins.

The LCO hydrotreatment results of NiW/AUSY-2 and a commercial catalyst are summarized in Table 6. The LCO used in this experiment, characterized by a high sulfur content, high aromatic content, and low cetane number, is a typical inferior feedstock for hydrotreatment. NiW/AUSY-2 and the commercial catalyst show comparable HDS and HDN conversion and diesel yields. However, NiW/AUSY-2 shows a higher HDA conversion than the commercial catalyst. Hence, the cetane number of the diesel product treated by NiW/AUSY-2 increases by 14 units in comparison with the FCC LCO feedstock. That of the commercial catalyst is only 11.5 units. Due to its high ring-opening activity, NiW/AUSY-2 is likely to convert polyaromatics to alkylbenzenes and alkylcycloalkanes with high cetane numbers.

4. Conclusion

NiW/AUSY-2 exhibited high ring-opening activity during the coupled hydrogenation and ring-opening of tetralin and hydrotreatment of LCO. This can be reasonably attributed to the advantages arising from the cooperation between metal sulfides and acid sites. First, USY-2 zeolite has medium acidity, which allows for good ring-opening activity and limits over-cracking. Second, NiW/AUSY-2 presents a high number of WS_2 layers, leading to high aromatic hydrogenation activity.

Acknowledgments

The authors thank Professor Xuanwen Li of Peking University for fruitful discussions. The authors wish to thank National Natural Science Foundation of China (Grant No. 20876171) and PetroChina for financial support.

References

[1] R.C. Santana, P.T. Do, M. Santikunaporn, W.E. Alvarez, J.D. Taylor, E.L. Sughrue, D.E. Resasco, Fuel 85 (2006) 643.
[2] G. Suppes, Z. Chen, Y. Rui, M. Mason, J. Heppert, Fuel 78 (1999) 73.
[3] C. Knottenbelt, Catal. Today 71 (2002) 437.
[4] C. Song, X. Ma, Appl. Catal. B 41 (2003) 207.
[5] G. McVicker, M. Daage, M. Touvelle, C. Hudson, D. Klein, W. Baird, J. Catal. 210 (2002) 137.
[6] C.G. Walter, B. Coq, F. Figueras, M. Boulet, Appl. Catal. A 133 (1995) 95.
[7] J.L. Carter, J.A. Cusumano, J.H. Sinfelt, J. Phys. Chem. 70 (1966) 2257.
[8] H. Zimmer, Z. Paal, J. Mol. Catal. 51 (1989) 261.
[9] D. Kubicka, N. Kumar, P. Mäki-Arvela, M. Tiitta, V. Niemi, T. Salmi, D.Y. Murzin, J. Catal. 222 (2004) 65.
[10] W. Li, Z. Wang, M. Zhang, K. Tao, Catal. Commun. 6 (2005) 656.
[11] M. Santikunaporn, J.E. Herrera, S. Jongpatiwut, D.E. Resasco, W.E. Alvarez, E.L. Sughrue, J. Catal. 228 (2004) 100.
[12] H.S. Cerqueira, P.C. Mihindou-Koumba, P. Magnoux, M. Guisnet, Ind. Eng. Chem. Res. 40 (2001) 1032.
[13] A. Corma, V. Gonzalez-Alfaro, A.V. Orchillés, J. Catal. 200 (2001) 34.
[14] T. Sugii, Y. Kamiya, T. Okuhara, Appl. Catal. A 312 (2006) 45.
[15] M.A. Arribas, P. Concepción, A. Martinez, Appl. Catal. A 267 (2004) 111.
[16] E. Rodriguez-Castellon, J. Merida-Robles, L. Diaz, P. Maireles-Torres, D.J. Jones, J. Roziere, A. Jimenez-Lopez, Appl. Catal. A 260 (2004) 9.
[17] E. Rodrguez-Castellon, L. Daz, P. Braos-Garca, J. Merida-Robles, P. Maireles-Torres, A. Jimenez-Lopez, A. Vaccari, Appl. Catal. A 240 (2003) 83.
[18] K. Sato, Y. Iwata, Y. Miki, H. Shimada, J. Catal. 186 (1999) 45.
[19] K. Sato, Y. Iwata, T. Yoneda, A. Nishijima, Y. Miki, H. Shimada, Catal. Today 45 (1998) 367.
[20] H. Yasuda, T. Sato, Y. Yoshimura, Catal. Today 50 (1999) 63.
[21] L. Ding, Y. Zheng, Z. Zhang, Z. Ring, J. Chen, J. Catal. 241 (2006) 435.
[22] L. Vradman, M.V. Landau, M. Herskowitz, Fuel 82 (2003) 633.
[23] P. Baeza, M. Villarroel, P. Avila, A. Lspez-Agudo, B. Delmon, F.J. Llambmas, Appl. Catal. A 304 (2006) 109.
[24] R.G. Tailleur, Fuel 87 (2008) 2551.
[25] M.A. Arribas, A. Martnez, Appl. Catal. A 230 (2002) 203.